HHS Public Access

Author manuscript

Mol Cancer Ther. Author manuscript; available in PMC 2016 July 01.

Published in final edited form as:

Mol Cancer Ther. 2015 July ; 14(7): 1680–1692. doi:10.1158/1535-7163.MCT-15-0080.

BRAF inhibition decreases cellular glucose uptake in melanoma in association with reduction in cell volume

Nicholas Theodosakis[1], **Matthew A. Held**[1], **Alexander Marzuka-Alcala**[2], **Katrina M. Meeth**[1], **Goran Micevic**[1], **Georgina V. Long**[3,5], **Richard A. Scolyer**[3,4], **David F. Stern**[1], and **Marcus W. Bosenberg**[1,2]

[1]Department of Pathology, Yale School of Medicine, New Haven, CT

[2]Department of Dermatology, Yale School of Medicine, New Haven, CT

[3]Melanoma Institute of Australia, Sydney, NSW, Australia

[4]Discipline of Pathology, The University of Sydney, Sydney, NSW, Australia

[5]Discipline of Medicine, The University of Sydney, Sydney, NSW, Australia

Abstract

BRAF kinase inhibitors have dramatically impacted treatment of *BRAF*$^{V600E/K}$-driven metastatic melanoma. Early responses assessed using [^{18}F]fluorodeoxyglucose uptake-positron emission tomography (FDG-PET) have shown dramatic reduction of radiotracer signal within two weeks of treatment. Despite high response rates, relapse occurs in nearly all cases, frequently at sites of treated metastatic disease. It remains unclear whether initial loss of ^{18}FDG uptake is due to tumor cell death or other reasons. Here we provide evidence of melanoma cell volume reduction in a patient cohort treated with BRAF inhibitors. We present data demonstrating that BRAF inhibition reduces melanoma glucose uptake per cell, but that this change is no longer significant following normalization for cell volume changes. We also demonstrate that volume normalization greatly reduces differences in transmembrane glucose transport and hexokinase-mediated phosphorylation. Mechanistic studies suggest that this loss of cell volume is due in large part to decreases in new protein translation as a consequence of vemurafenib treatment. Ultimately, our findings suggest that cell volume regulation constitutes an important physiologic parameter that may significantly contribute to radiographic changes observed in clinic.

Keywords

Cell Volume; glucose uptake; melanoma

Reprints should be sent to Nicholas Theodosakis, Dermatology, PO Box 208059, 333 Cedar Street, New Haven, CT 06520-8059.

The authors disclose no potential conflicts of interest

Financial Information: These studies were supported in part by grants from the NIH: Yale SPORE in Skin Cancer, funded by the National Cancer Institute P50 CA121974 to R. Halaban, and Ruth L. Kirschstein NRSA 1F30CA180591-01 funded by the National Cancer Institute to N. Theodosakis. The study was also funded by an American Skin Association Student Grant to N. Theodosakis and the Yale Cancer Center to M.W. Bosenberg.

Introduction

Cancer cells frequently display high rates of fermentative glycolysis relative to benign cells under normoxic conditions(1–3), a characteristic often referred to as “aerobic glycolysis” that involves increased consumption of glucose. The benefits of this include increased precursors for macromolecule synthesis, generation of reducing agents, and production of adequate ATP for growth(4–7). Evidence of aerobic glycolysis can be observed clinically using the glucose analog radiotracer 18-fluorodeoxyglucose (^{18}FDG) with positron emission tomography (PET) imaging, reflecting a relative increase in glucose uptake in tumors compared to most normal tissues. It is often used in tandem with tumor dimensional measurements, with classification of therapeutic responses defined by a set of guidelines known as Response Evaluation Criteria in Solid Tumors (RECIST) based on changes in the sum of the longest diameters of all CT or MRI-measured lesions. Interestingly, during the initial phases of targeted therapy, the FDG-PET response may be greater than the degree of tumor shrinkage noted with CT imaging(8). Together, FDG-PET and RECIST serve as useful methods for tracking the efficacy of therapies in primary and metastatic tumors(9, 10). This occurs dramatically in melanoma tumors driven by oncogenic BRAF treated with BRAF inhibitors such as vemurafenib and dabrafenib (8, 11–13).

Approximately half of human melanomas harbor activating mutations at amino acid V600 in the protein kinase BRAF, leading to constitutive activation of the mitogen-activated protein kinase (MAPK) pathway(14, 15). The BRAF inhibitors vemurafenib and dabrafenib suppress downstream activity of the MAPK pathway in the majority of *BRAF*-mutant tumors(16, 17). Patients treated with vemurafenib or dabrafenib typically show decreased FDG-PET signal within two weeks, often before significant reduction in tumor mass(8, 13). In roughly 40% of patients, less than 30% maximal tumor shrinkage is ultimately observed on therapy, yet most tumors will have markedly decreased FDG-PET signal with a progression-free survival benefit(12). Subsequent increases in ^{18}FDG uptake in treated tumors tightly correlate with emergence of resistance to vemurafenib, occurring between 2 and 18 months in most patients(11). Curiously, many tumors that become PET negative on therapy often regain ^{18}FDG positivity later in the same location, likely signifying recurrence of residual disease at those sites. Both the precise mechanism for this early decrease and the mechanism behind subsequent increase of glucose uptake at relapse have yet to be conclusively determined.

In cancer cells, transmembrane GLUT carrier proteins that facilitate diffusion across the plasma membrane(18), and hexokinase enzymes I–IV(19), which phosphorylate glucose in the cytosol, are known to contribute to ^{18}FDG trapping. Only HKI and HKII are expressed to a significant degree in melanoma(20). HKII is known to support aerobic glycolysis, with its activity varying in response to changing glucose levels(21). HKII is also tied to regulation of apoptosis through binding to the mitochondrial membrane porin VDAC(22). Interestingly, high levels of HKII have been observed in a variety of actively proliferating cancer cells(21, 23). While reduction of glucose uptake with BRAF inhibitors in melanoma has been noted(5, 11, 24), previous mechanistic explanations have focused mainly on changes in GLUT-mediated transport (24), with studies specifically investigating changes in HK levels mostly confined to MEK inhibitors(25). Here we investigate how the metabolic

and morphological properties of melanoma cells on therapy interact to produce the observed changes in ^{18}FDG uptake.

Materials and Methods

Human Melanoma Tissue samples

Paired excision biopsies of 10 pre-treatment (PRE) and corresponding early during-treatment (EDT) biopsies at 3 and 15 days after initiation of BRAF inhibitor therapy were obtained in patients with *BRAF*-mutant metastatic melanoma as previously described(8, 16). Maximum standardized uptake values (SUVmax) from ^{18}FDG-PET imaging were obtained on day 15 of treatment(8) when available. Apoptotic cell counts represent average numbers of pyknotic tumor cells across 5 different 1 mm^2 areas per slide. Pyknotic cells were defined by hyperchromatic and shrunken nuclei with cytoplasmic compaction. Areas of ischemic, geographic necrosis were not included.

Cell Culture and Generation of Acquired Resistant Lines

All specimens were collected with patients' informed consent in accordance with the Health Insurance Portability and Accountability Act (HIPAA) under a Human Investigations Committee protocol. Authentication and mutational status were confirmed via expression profiling and Sanger sequencing as described previously(26). Cell lines were grown in OPTI-MEM (Invitrogen, Carlsbad, CA, USA) supplemented with 1% penicillin-streptomycin and 10% fetal bovine serum maintained in a 37°C incubator maintained at 5% CO_2. All lines utilized were derived from surgical melanoma resections and were provided by Dr. Ruth Halaban (Yale University, New Haven, CT, USA)(27) as part of the YSPORE tissue bank and passaged less than 6 months. Parental YUMAC and YUSIT1 lines were continuously grown in vemurafenib (up to 5 μM) until they exhibited resistance to growth inhibition by vemurafenib and were designated YUMACr and YUSIT1r. Parental lines were re-designated YUMACs and YUSIT1s. Acquired resistance was verified over a 72 hour time period and quantified using the CyQUANT® NF Cell Proliferation Assay Kit (Life Technologies, Carlsbad, CA, USA).

Cell Size Analysis

Cell median diameter of non-adherent cells was calculated using a Z2 Coulter Counter (Beckman Coulter, Inc., Indianapolis, IN) calibrated with polystyrene size-standardized beads (Spherotech, Lake Forest, IL). Volumes of spherical cells in suspension were calculated from these measurements. Adherent cell area, both *in vitro* and from paraffin-embedded sections, was calculated by polygonal selection using ImageJ (v. 1.46r, NIH, Bethesda, MD) using 20 separate cells judged to be representative of the entire population. Patient sample images were taken using a Olympus BX41 microscope equipped with an optical micrometer.

^{3}H-O-methylglucose transmembrane glucose transport assay

To quantify transmembrane glucose transport, we adapted a previous protocol using the non-phosphorylatable tritiated glucose analog 3-O-methylglucose (3-OMG)(28). Cells were counted by hemocytometer and resuspended in glucose-free DMEM supplemented with

varying concentrations of glucose along with a ratio of 1.8 μCi of 3-OMG (PerkinElmer, Waltham, MA, USA) per mmol glucose for varying lengths of time. Uptake was halted with a quenching cocktail of 300μM phloretin (Sigma-Aldrich, St. Louis, MO, USA). Four washes were performed with the quenching cocktail before the residual pellet was lysed and added to Ultima Gold™ Scintillation Cocktail (PerkinElmer). Counts per minute were assessed with a Beckman Coulter LS 6500 Liquid Scintillation Counter (Beckman Coulter, Ramsey, MN, USA). Cell number was also corrected for using the CyQUANT® NF Cell Proliferation Assay after washing. Results were also corrected for cell size using triplicate measurements of cell volume by Coulter Counter as described above.

Hexokinase activity assay

Total cellular hexokinase activity was assessed using an existing protocol(29), adapted from an earlier protocol(30). Cells were counted by hemocytometer. A volume of lysate containing 2.5×10^5 cells or 30μg of total protein was then added to a 96 well optical plate (Thermo Fisher Scientific, Waltham, MA, USA) followed by an assay cocktail composed of 50mM triethanolamine buffer, 19 mM Adenosine 5′-Triphosphate Solution, 100 mM magnesium chloride, 14 mM β-nicotinamide adenine dinucleotide phosphate, 125 units/mL glucose-6-phosphate dehydrogenase enzyme solution, and varying concentrations of glucose. Plates were read using a Spectramax M3 microplate reader (Molecular Devices, Sunnyvale, CA, USA) and maximum velocities computed using SoftMax Pro 6.2.2 (Molecular Devices). Correction for alterations in protein content per cell was performed using results of the Bradford assay in triplicate or CyQUANT® NF Cell Proliferation Assay.

Flow Cytometry

To measure glucose uptake, pellets were then resuspended in PBS supplemented with 300 μM 2-deoxy-2-[(7-nitro-2,1,3-benzoxadiazol-4-yl)amino]-D-glucose (2-NBDG) (Cayman Chemical, Ann Arbor, MI, USA) for 10 minutes. After a single wash, pellets were stained using the BD Pharmingen Apoptosis Detection Kit II according to the manufacturer's protocol (BD Biosciences, Franklin Lakes, NJ, USA). Samples were analyzed with the BD LSRII flow cytometer to at least 10,000 events per sample. Compensation for spectral overlap between 2-NBDG and propidium iodide was applied for each experiment. Each line was treated independently, and gates were fixed based on negative control signals. Plots were generated using FlowJo 9.6.2.

Immunoblotting

Immunoblots were conducted with the following primary antibodies all used at 1:1000: Hexokinase II (cat. no. 2867; Cell Signaling Technology, Danvers, MA, USA), Beta Actin (cat. no. 4970; Cell Signaling), Beta Tubulin (cat. no. 2128; Cell Signaling), GSK3B (cat. no. 9315), p-GSK3B S9 (cat. no. 9323; Cell Signaling), p-p90RSK T573 (cat. no. 9346; Cell Signaling), RSK1/RSK2/RSK3 (cat. no. 9355; Cell Signaling), hsp60 (cat. no. sc-1052; Santa Cruz Biotechnology, Santa Cruz, CA, USA), GLUT1 (cat. no. 07-1401; Millipore, Billerica, MA, USA), GLUT3 (cat. no. NBP1-89762; Novus Biologicals, Littleton, CO, USA) and the secondary antibody Anti-rabbit IgG, HRP-linked Antibody (cat. no. 7074S; Cell Signaling).

Radiographic Studies

After drug treatment, cells were incubated in cysteine and methionine-free DMEM (Life Technologies, Carlsbad, CA, USA) for one hour before one hour incubation with the same media supplemented with EasyTag™ EXPRESS^{35}S Protein Labeling Mix (PerkinElmer, Waltham, MA, USA). After lysate collection with or without immunoprecipitation, samples were separated by SDS-PAGE and read using a Storm 860 phosphorimager (GMI Inc., Ramsey, MN, USA).

RNA extraction and quantitative PCR

Total RNA was extracted using an RNeasy Mini Kit (Qiagen, Venlo, Netherlands) and reverse transcribed using a Transcriptor First Strand cDNA Synthesis Kit (Roche, Basel, Switzerland) using both Oligo dT and random hexamers. Quantitative PCR was carried out using FastStart Universal SYBR Green Master (Rox) (Roche) relative to GAPDH levels on a StepOnePlus™ Real-Time PCR System (Life Technologies, Carlsbad, CA, USA) and fold changes were calculated using StepOne Software v 2.0.

Results

Cellular volume reduction occurs in clinical melanoma samples in response to BRAF inhibition

Maximum standardized uptake values (SUVmax) from ^{18}FDG-PET imaging in our paired biopsy pre-treatment (PRE) and early during treatment (EDT) cohort were obtained on day 15 of therapy(8, 16). Evaluation of cellular size in the samples demonstrated a significant decrease in cellular and cytoplasmic volume following initiation of BRAF inhibitor therapy (Figure 1A and 1B) without a significant decrease in average number of nuclei per tumor cross sectional area (Figure 1C). Contraction of cytosolic volume without loss of nuclei consequentially led to an increase in average intercellular distance in most patients (Figure 1D). There was not an associated increase in the average number of apoptotic cells per mm^2 in the majority of cases (Figure 1E).

BRAF inhibition alters glucose uptake in melanoma

After noting the morphological changes, we evaluated changes in glucose metabolism *in vitro* to determine if the phenotypes are linked. To quantify total glucose uptake changes *in vitro*, we incubated patient-derived melanoma cell lines harboring activating mutations in *BRAF* with 2-[N-(7-nitrobenz-2-oxa-1,3-diazol-4-yl) amino]-2-deoxy-D-glucose (2-NBDG), a non-radioactive, fluorescent, non-metabolizable form of glucose similar to [^{18}F]fluorodeoxyglucose, that is trapped within cells upon phosphorylation by hexokinase(31). Melanoma lines sensitive to vemurafenib, defined elsewhere as showing at least 50% growth inhibition at or below 3 μM drug(26) showed a significant decrease in 2-NBDG uptake per cell measured by flow cytometry after 12 hour exposure to vemurafenib, with maximum reduction in median fluorescent intensity (MFI) observed by 72 hours (Figure 2A). This was not associated with a significant increase in cell death as measured by annexin-V and propidium iodide flow cytometry (Supplemental Figure 1A).

Patients with acquired resistance to mutant BRAF inhibitors show elevated SUVmax, relative to normal tissue even on BRAF inhibitors(11). To investigate this characteristic, we generated acquired vemurafenib-resistant clones by chronically growing two sensitive lines in vemurafenib and assessing 2-NBDG uptake. Drug resistance was verified by determination of IC_{50} for proliferation at 72 hours (Supplemental Figure 1B, 1C). As expected, 2-NBDG uptake in acquired resistant cell lines was maintained in the presence of vemurafenib (Figure 2B). Moreover, intrinsically vemurafenib-resistant mutant *BRAF*-driven melanoma lines and non-*BRAF* mutant lines, showed equivalent or enhanced 2-NBDG uptake relative to vemurafenib-sensitive lines (Figure 2C, Supplementary Table 1). These *in vitro* observations suggest that sensitivity to vemurafenib is closely associated with glucose uptake per cell, and phenocopies what is seen by ^{18}FDG imaging in melanoma tumors from patients. Moreover, we observed that glucose uptake in sensitive lines was completely restored 72 hours after removal of vemurafenib, further suggesting that glucose uptake loss is a reversible effect of BRAF inhibition rather than a result of apoptosis (Figure 2D). These results demonstrate that vemurafenib greatly reduces glucose uptake per cell within 72 hours of incubation with drug.

Vemurafenib-induced reduction in glucose uptake is not accounted for by alterations in transmembrane glucose transport

The intracellular trapping of 2-NBDG after phosphorylation by hexokinase precludes its use as an accurate indicator of GLUT function. Therefore we utilized the non-phosphorylatable tritiated glucose analog 3-O-methylglucose (3-OMG) in order to quantify transport rate changes independent of hexokinase activity. Normalizing to cell count, we observed a mild decrease in uptake in vemurafenib-treated vemurafenib-sensitive cell lines that was not observed in acquired vemurafenib resistant cells (Figure 3A). This was not associated with reduced protein levels of two of the major GLUT transporter enzymes known to be highly active in melanoma, GLUT1 and GLUT3(32) (Figure 3B). Accordingly, we did not observe a significant change in transporter mRNA levels in sensitive or resistant lines (Figure 3C). These data indicated that changes in overall glucose transport are insufficient to explain the decrease in glucose uptake in these BRAF-inhibited cells.

Reduction of hexokinase II protein and overall hexokinase activity per cell is observed in sensitive but not acquired resistant melanoma lines treated with vemurafenib

We next investigated whether reduced hexokinase activity contributes to BRAF inhibitor induced reduction in cellular 2-NBDG levels. We first performed an *in vitro* total hexokinase activity assay in sensitive and resistant lines, normalizing to cell count. Vemurafenib-sensitive lines showed a significant decrease in hexokinase activity per cell after 72 hour vemurafenib treatment, in contrast to acquired vemurafenib-resistant derivatives, which showed no significant change (Figure 4A). Consistent with previous literature identifying HKII as the isoenzyme most intimately tied to cellular growth and proliferation of tumor cells(21),(23), we observed reduction of HKII protein starting at approximately 6–8 hours. Marked reduction of HKII levels was seen by 72 hours in sensitive lines (Figure 4B), which corresponded with the decrease in glucose uptake observed by 2-NBDG flow cytometry. Melanoma lines with acquired resistance to

vemurafenib or those without *BRAF* mutations showed no significant differences in HKII protein levels upon BRAF inhibition (Figure 4C).

Quantitative measurement of HKII mRNA showed virtually no change after 72 hours of vemurafenib treatment in sensitive or resistant lines (Supplementary Figure 2A), suggesting a post-transcriptional mechanism of HKII loss. We observed a significant loss of HKII protein in innately vemurafenib-resistant lines YUKSI and YUKOLI comparable to sensitive lines (Figure 4D), despite the increased uptake of 2-NBDG observed by flow cytometry (Figure 1C). We hypothesized that a compensatory increase in other HK isoforms present in intrinsic resistant lines might be responsible for the increase of glucose uptake. Interestingly, we found that both vemurafenib-sensitive and intrinsically resistant lines showed a significant rise in HKI levels at 72 hours (Figure 4E). In contrast, all acquired vemurafenib-resistant lines as well as non-*BRAF* mutant lines showed no significant change in HKI levels (Figure 4F), underscoring the complex relationship between changes in HK levels and 2-NBDG uptake with BRAF inhibition (Figure 4G). Furthermore, immunohistochemical staining of our biopsy cohort for HKII revealed moderate to high levels in all cases but revealed no significant difference between levels in PRE and EDT samples (Supplementary Figure 2B). These conflicting data suggest that changes in HK activity and regulation with vemurafenib treatment do not show a consistent relationship with glucose uptake, hinting that an additional alteration might be responsible for clinical therapeutic responses.

Cell volume decrease predicts extent of reduction of glucose uptake *in vitro*

SUVmax alterations measured by ^{18}FDG-PET account for the total radioactive signal emitted from a tumor with a particular gross tumor volume. These measurements do not distinguish between the relative proportions of cell volume and extracellular matrix and edema that comprise the tumor microenvironment. As cellular volume is another major determinant of total solute movement into a cell, including glucose, we microscopically examined morphological changes in a wide range of melanoma lines using the cell volume measurement functions of a Z2 Coulter Counter. Over multiple cases, we quantified an average volume decrease of 43% across three highly vemurafenib-sensitive lines: YUMACs, YUSIT1s, and YUGEN8, but there was no substantial change in cell volume in lines resistant to BRAF inhibition (Figure 5A and 5B). Moreover, we observed that the intrinsically vemurafenib-resistant lines YUKSI and YUKOLI, which showed mild increase in 2-NBDG uptake with BRAF inhibition, also showed increases in median cell volume. Mean adherent area calculations also supported these trends (Supplemental Figure 3). Ultimately, when calculated across 13 melanoma lines, changes in cell volume following vemurafenib treatment were found to predict 83% of the variance in NBDG uptake in our model (Figure 5C, $p < 0.001$, Student's t-test). This relationship also showed a strong correlation with vemurafenib concentrations required to inhibit growth of cells by 50% (GI_{50}), with GI_{50} in our model predicting 86% of the variance in volume change (Figure 5D, $p<0.001$, Student's t test). We found the same relationship between cell volume and uptake changes when cells were treated with the MEK inhibitor AZD-6244 (Supplemental Figure 4A and 4B), an effect not explained by cell cycle arrest alone (4C and 4D). Applying correction for changes in cell volume to calculated transmembrane glucose transport

(radiolabeled 3-OMG uptake) greatly reduced the perceived decrease in glucose transport kinetics (Figure 5E). Similarly, normalization to protein content, as opposed to cell number, greatly reduced differences in pan-HK activity seen in treated versus untreated cells (Figure 5F). Taken together, these data strongly suggest that measured alterations in glucose transport and phosphorylation are markedly influenced by cell volume changes.

Extrinsic regulation of cell size regulates cellular glucose uptake independent of BRAF inhibition

To establish a mechanistic link between cell volume changes and glucose uptake independent of metabolic changes from vemurafenib, we increased cell volume by decreasing solution tonicity. We found that decreasing the overall solution tonicity by 50% and 75% during 2-NBDG incubation significantly increased cell volume as measured by Coulter Counter (Figure 6A). We also found that changing incubation tonicity concomitantly increased 2-NBDG uptake (Figure 6B) under otherwise identical conditions without significant cell death or membrane disruption (Supplemental Figure 5). These findings suggest that changes in cell size alone are sufficient to alter glucose uptake in melanoma. Extending these findings to BRAF inhibited cells, we found that incubating cells exposed to vemurafenib for 72 hours in hypotonic 2-NBDG solutions was sufficient to rescue glucose uptake relative to untreated controls incubated at normal tonicity (Figure 6C). As a second method for verification of this concept, we treated cells for 24 hours with 50 μg/mL of the ribosomal translation inhibitor cycloheximide (CHX). CHX treatment of vemurafenib-sensitive cells produced a decrease in both cell volume (Figure 6D) and glucose uptake (Figure 6E) that was comparable to the decrease induced by vemurafenib. CHX treatment in acquired or primary vemurafenib-resistant lines also resulted in marked reduction of cell volume and 2-NBDG uptake that was significantly greater than vemurafenib treatment in these lines. CHX treatment of additional lines revealed a positive linear correlation between cell volume and 2-NBDG uptake (Figure 6F). Recent studies have demonstrated strong links between cell volume and changes in total cellular protein content(19, 33), as well as significant inhibition of 5′ cap-dependent translation with BRAF inhibition(34, 35). These studies, in addition to our CHX data, suggested that changes in cap-dependent protein translation may be at least partially responsible for the noted decrease in cell size and glucose uptake loss. Consistent with this conclusion, we also noted a decrease in HKII levels with CHX treatment that was comparable to that induced by vemurafenib (Figure 6G), as well as a significant decrease in overall protein synthesis after 72 hours of drug treatment (Figure 6H). This underlying mechanism was also supported by studies showing significant inhibition of assembly of the cap-dependent translation initiation complex, as well as decreased HKII de novo translation (Supplemental Figure 6A and 6B). In parallel, dephosphorylation of ribosomal protein p70S6K and S6 downstream of mTOR, both of which are involved in initiation complex assembly and activity(36), occurs within 24 hours of treatment, mirroring observed alterations in cell volume and protein content (Supplemental Figure 7). Additional loss of S6 and p70S6K continues out to 72 hours, with later loss of upstream Akt phosphorylation, further paralleling increasing loss of glucose uptake and volume over this timeframe (Supplemental Figure 8). In line with previous studies(37), loss of S6 phosphorylation was greatly abrogated in resistant lines, showing a consistent relationship between drug sensitivity, volume, new protein synthesis, and S6

activity. The importance of decreases in protein translation over increased protein degradation was also supported through the inability of the proteasome inhibitors bortezomib or MG132 to significantly rescue HKII loss (Supplemental Figure 9). This suggests that targeted destruction of HKII at the proteasome is not primarily responsible for the observed decreases in HKII levels.

Discussion

RECIST criteria are currently widely utilized to evaluate therapy efficacy. Though response rates are defined by the sum of complete and partial responses, it is also apparent that patients with stable disease may derive progression free and overall survival benefit from treatment(12). Poor correlation between tumor shrinkage over an initial time window and overall survival is frequently seen in the melanoma immunotherapy, where increases in tumor size can occur before eventual complete regression with survival benefit(6, 38). This suggests that therapy-induced changes in tumor volume taken in isolation may not be the optimal predictor of patient survival. Incorporation of additional data may be needed, necessitating improved understanding of the mechanism of tumor shrinkage.

Though induction of apoptosis has been assumed to be a principal mechanism of action of BRAF inhibitors, there is relatively little evidence that this is the primary mode of effective response in patients. At odds with extensive cell death is the lack of observation of tumor lysis syndrome in several large clinical trials of BRAF inhibitors(1, 2, 9, 10), which might be expected from toxic chemotherapy treatments producing comparable RECIST responses. Evaluation of a series of melanoma patients early during treatment (EDT) demonstrated that geographic tumor necrosis occurred at a higher rate than observed in pre-treatment biopsies(8), however geographic necrosis is typically secondary to vascular insufficiency (ischemia or infarct). A clear increase in individual apoptotic cells was not observed. In contrast, significant decrease in proliferation (Ki67) and Cyclin D1 levels noted in previous staining of a subset of this cohort suggest G_0/G_1 arrest(8). In vitro, high doses of BRAF inhibitors typically induce low levels of apoptosis (0–10%), with some cell lines (e.g. A375) exhibiting higher rates. In essentially all *BRAF*-mutant lines, resistant clones emerge following chronic treatment *in vitro*, mimicking the high rate of relapse in melanoma patients treated with BRAF inhibitors. Based on these data, tumor shrinkage is likely a complex phenomenon that integrates occasional geographic (ischemic) necrosis, cell cycle arrest, and a minor component of apoptotic cell death. The sum of these factors does not appear to fully account for and correlate with clinical tumor shrinkage in BRAF inhibitor-treated melanoma patients.

Here we provide evidence for BRAF inhibitor-induced reduction in cell volume as a contributing factor in clinical tumor shrinkage and FDG-PET responses. We observed a significant decrease in cell size in melanoma patient samples EDT, and a trend toward correlation between magnitude of shrinkage and SUVmax decrease. The observed similar level of HKII staining, reduction in cytoplasmic volume, and increase in intercellular distance early during treatment suggests that decrease in cell size precedes the slow, gradual reduction in tumor size that is typically observed. These findings suggest that early/rapid decrease in FDG-PET signal without corresponding tumor shrinkage as determined by CT

imaging may be due to decreased tumor cellular mass per imaging voxel, intermixed with increased edematous changes. Resolution of the extracellular edematous changes would be predicted to result in gradual tumor shrinkage associated with residual to slightly elevated FDG-PET signal, which is typically observed. On a broader scale, these findings raise the possibility that imaging-based responses to targeted signal transduction inhibitors may be partially mediated by modulation of cell volume in addition to cell death.

Recent studies have suggested that MAPK inhibition may influence glucose metabolism in *BRAF*$^{V600E/K}$ mutant cells by inducing decreases in GLUT transporter or HKII protein levels(5, 11, 24, 25). Decreased metabolic activity has also been observed in the form of decreased lactate production(25), oxygen consumption(39), and metabolic enzyme expression(24): all generally normalized to protein mass or cell count. In this study, we provide evidence in melanoma that cell size alone can significantly regulate glucose uptake in *BRAF*-mutant melanomas treated with vemurafenib. We did note decreases in glucose uptake and HK activity per cell, however, following additional normalization for cell volume, the changes in HK activity were markedly diminished. This suggests that while previously demonstrated metabolic enzyme changes do contribute, they are likely to be only a part of the mechanism for ^{18}FDG signal loss. This finding may also help explain the metabolic changes induced by BRAF inhibition in previous reports (11, 24, 25, 40) which have largely focused on changes in the first 24 hours after induction of therapy without exploration of later steady state. Taken together, these findings emphasize a broader need for consideration of cell size changes in metabolic and biochemical studies, especially in melanoma biology, where cell populations may consist of multiple subclones with heterogeneous morphological properties(16, 20).

In this study, we demonstrate an increase in HKI levels in all melanoma cell lines that show HKII decrease. This could suggest that HKI may help compensate for changes in HKII in melanoma to maintain glycolytic activity, as indicated by our evaluation of overall HK activity, and consistent with previous studies in breast and lung cancer(23). Interestingly, we found that intrinsically vemurafenib resistant melanomas show a mild increase in glucose metabolism and decrease in proliferation with treatment, yet display the same HKII/HKI switch seen in sensitive *BRAF*-mutant melanomas. Further studies will be required to determine the functional effects of upregulation of HKI, as well as the functional contributions of individual HK isoforms to glucose uptake.

Evidence provided by this study suggests that total protein translation per cell is significantly decreased with BRAF inhibition, in agreement with other studies(34, 35). This occurs in parallel with vemurafenib-induced decreases in p70S6K and S6 activity observed previously(37), and is largely absent in lines that have acquired resistance to the drug. The synchronicity of loss of cell volume, decrease in protein translation, and downregulation of p70S6K and S6 activity, as well as the correlation of these phenomena with drug sensitivity, further support the proposed explanation for decreases in glucose uptake. Our findings also expand on previous melanoma metabolomics literature, providing a mechanistic explanation for the previously noted downregulation of multiple key metabolic enzymes(24, 25). Furthermore, our study provides evidence for the importance of global protein synthesis to maintenance of cell size, and the consequences for the clinically-relevant characteristic of

glucose uptake capacity when this process becomes dysregulated, emphasizing the previously established relationship between cell size, cell cycle progression, and translation[20, 34]. Indeed, the G_0/G_1 cell cycle arrest and markedly reduced BrdU incorporation we observed in vemurafenib-treated cells also suggests that new nucleic acid production is also greatly decreased in the setting of BRAF inhibition; a finding which may reflect broader changes in glucose carbon utilization that merits further exploration. Nevertheless, the inability of cell cycle arrest to independently fully account for decreased size and glucose uptake suggests that additional MAPK-specific regulation of translation and volume maintenance are also being inhibited. These findings taken together suggest a quiescent metabolic phenotype, implying that inhibition of mutant BRAF removes the driving force behind neoplastic growth and metabolism without destabilizing cells enough to cause apoptosis, levels of which have previously been noted to be variable and frequently minimal(39, 41).

In summary, our study suggests that cell size is an important determinant of glucose uptake in melanoma and can affect many of the observed changes in metabolic activity. It also provides a possible explanation for the re-emergence of resistant tumors at sites identical to previous metastases. Furthermore, these findings underscore the importance of correcting for physical parameters when undertaking studies in cellular metabolism, as well as the dynamic interplay between growth, metabolism, and signaling.

Supplementary Material

Refer to Web version on PubMed Central for supplementary material.

Acknowledgments

We would like to acknowledge Ruth Halaban and Antonella Bacchiochi for providing melanoma cell lines from the Yale melanoma SPORE tissue bank, as well as Casey Langdon for helping to develop cell lines with acquired resistance to BRAF inhibition.

Abbreviations

HKI	hexokinase I
HKII	hexokinase II

References

1. McArthur GA, Chapman PB, Robert C, Larkin J, Haanen JB, Dummer R, et al. Safety and efficacy of vemurafenib in BRAF(V600E) and BRAF(V600K) mutation-positive melanoma (BRIM-3): extended follow-up of a phase 3, randomised, open-label study. The lancet oncology. 2014; 15:323–32. [PubMed: 24508103]
2. Falchook GS, Long GV, Kurzrock R, Kim KB, Arkenau TH, Brown MP, et al. Dabrafenib in patients with melanoma, untreated brain metastases, and other solid tumours: a phase 1 dose-escalation trial. Lancet. 2012; 379:1893–901. [PubMed: 22608338]
3. Koppenol WH, Bounds PL, Dang CV. Otto Warburg's contributions to current concepts of cancer metabolism. Nature reviews Cancer. 2011; 11:325–37.
4. PDA. Energy metabolism in cancer cells: How to explain the Warburg and Crabtree effects? Med Hypotheses. 2012; 79:388–92. Epub 2012 Jul 5. [PubMed: 22770870]

5. Sondergaard JN, Nazarian R, Wang Q, Guo D, Hsueh T, Mok S, et al. Differential sensitivity of melanoma cell lines with BRAFV600E mutation to the specific Raf inhibitor PLX4032. Journal of translational medicine. 2010; 8:39. [PubMed: 20406486]
6. Hoos A, Parmiani G, Hege K, Sznol M, Loibner H, Eggermont A, et al. A clinical development paradigm for cancer vaccines and related biologics. Journal of immunotherapy (Hagerstown, Md: 1997). 2007; 30:1–15.
7. Scott DA, Richardson AD, Filipp FV, Knutzen CA, Chiang GG, Ronai ZA, et al. Comparative metabolic flux profiling of melanoma cell lines: beyond the Warburg effect. The Journal of biological chemistry. 2011; 286:42626–34. [PubMed: 21998308]
8. Long GV, Wilmott JS, Haydu LE, Tembe V, Sharma R, Rizos H, et al. Effects of BRAF inhibitors on human melanoma tissue before treatment, early during treatment, and on progression. Pigment cell & melanoma research. 2013; 26:499–508. [PubMed: 23557327]
9. Sosman JA, Kim KB, Schuchter L, Gonzalez R, Pavlick AC, Weber JS, et al. Survival in BRAF V600-mutant advanced melanoma treated with vemurafenib. The New England journal of medicine. 2012; 366:707–14. [PubMed: 22356324]
10. Chapman PB, Hauschild A, Robert C, Haanen JB, Ascierto P, Larkin J, et al. Improved survival with vemurafenib in melanoma with BRAF V600E mutation. The New England journal of medicine. 2011; 364:2507–16. [PubMed: 21639808]
11. Baudy ARDT, Flores-Mercado JE, Hoeflich KP, Su F, van Bruggen N, Williams SP. FDG-PET is a good biomarker of both early response and acquired resistance in BRAFV600 mutant melanomas treated with vemurafenib and the MEK inhibitor GDC-0973. EJNMMI Res. 2012; 2:22.10.1186/2191-219X-2-22 [PubMed: 22651703]
12. McArthur GAPI, Amaravadi R, Ribas A, Chapman P, Kim KB, Sosman JA, Lee RJ, Nolop K, Flaherty KT, Callahan J, Hicks RJ. Marked, homogeneous, and early [18F]fluorodeoxyglucose-positron emission tomography responses to vemurafenib in BRAF-mutant advanced melanoma. J Clin Oncol. 2012; 30:1628–34. Epub 2012 Mar 26. [PubMed: 22454415]
13. Carlino MS, Saunders CA, Haydu LE, Menzies AM, Martin Curtis C Jr, Lebowitz PF, et al. (18)F-labelled fluorodeoxyglucose-positron emission tomography (FDG-PET) heterogeneity of response is prognostic in dabrafenib treated BRAF mutant metastatic melanoma. European journal of cancer (Oxford, England: 1990). 2013; 49:395–402.
14. Davies H, Bignell GR, Cox C, Stephens P, Edkins S, Clegg S, et al. Mutations of the BRAF gene in human cancer. Nature. 2002; 417:949–54. [PubMed: 12068308]
15. Garnett MJ, Marais R. Guilty as charged: B-RAF is a human oncogene. Cancer cell. 2004; 6:313–9. [PubMed: 15488754]
16. Rizos H, Menzies AM, Pupo GM, Carlino MS, Fung C, Hyman J, et al. BRAF inhibitor resistance mechanisms in metastatic melanoma: spectrum and clinical impact. Clinical cancer research: an official journal of the American Association for Cancer Research. 2014; 20:1965–77. [PubMed: 24463458]
17. Ravnan MCMM. Vemurafenib in patients with BRAF V600E mutation-positive advanced melanoma. Clin Ther. 2012; 34:1474–86. Epub 2012 Jun 27. [PubMed: 22742884]
18. Killander D, Zetterberg A. A quantitative cytochemical investigation of the relationship between cell mass and initiation of DNA synthesis in mouse fibroblasts in vitro. Experimental cell research. 1965; 40:12–20. [PubMed: 5838935]
19. Mir M, Wang Z, Shen Z, Bednarz M, Bashir R, Golding I, et al. Optical measurement of cycle-dependent cell growth. Proceedings of the National Academy of Sciences of the United States of America. 2011; 108:13124–9. [PubMed: 21788503]
20. Wachsberger PR, Gressen EL, Bhala A, Bobyock SB, Storck C, Coss RA, et al. Variability in glucose transporter-1 levels and hexokinase activity in human melanoma. Melanoma research. 2002; 12:35–43. [PubMed: 11828256]
21. glucose SlohIaIdtmfo. Subcellular localization of hexokinases I and II directs the metabolic fate of glucose. PLoS One. 2011; 6:e17674. [PubMed: 21408025]
22. Arzoine LZN, Ben-Romano R, Shoshan-Barmatz V. Voltage-dependent anion channel 1-based peptides interact with hexokinase to prevent its anti-apoptotic activity. J Biol Chem. 2009; 284:3946–55. Epub 2008 Dec 2. [PubMed: 19049977]

23. Patra KC, Wang Q, Bhaskar PT, Miller L, Wang Z, Wheaton W, et al. Hexokinase 2 is required for tumor initiation and maintenance and its systemic deletion is therapeutic in mouse models of cancer. Cancer cell. 2013; 24:213–28. [PubMed: 23911236]
24. Parmenter TJ, Kleinschmidt M, Kinross KM, Bond ST, Li J, Kaadige MR, et al. Response of BRAF-Mutant Melanoma to BRAF Inhibition Is Mediated by a Network of Transcriptional Regulators of Glycolysis. Cancer discovery. 2014; 4:423–33. [PubMed: 24469106]
25. Falck Miniotis M, Arunan V, Eykyn TR, Marais R, Workman P, Leach MO, et al. MEK1/2 Inhibition Decreases Lactate in BRAF-Driven Human Cancer Cells. Cancer research. 2013
26. Held MA, Langdon CG, Platt JT, Graham-Steed T, Liu Z, Chakraborty A, et al. Genotype-selective combination therapies for melanoma identified by high-throughput drug screening. Cancer discovery. 2013; 3:52–67. [PubMed: 23239741]
27. Halaban R, Zhang W, Bacchiocchi A, Cheng E, Parisi F, Ariyan S, et al. PLX4032, a selective BRAF(V600E) kinase inhibitor, activates the ERK pathway and enhances cell migration and proliferation of BRAF melanoma cells. Pigment cell & melanoma research. 2010; 23:190–200. [PubMed: 20149136]
28. Yamamoto NUM, Sato T, Kawasaki K, Sawada K, Kawabata K, Ashida H. Measurement of glucose uptake in cultured cells. Curr Protoc Pharmacol. 2011; Chapter(Unit 12.4):1–22.
29. Enzymatic Assay of Hexokinase. [cited 2014; Available from: http://www.sigmaaldrich.com/technical-documents/protocols/biology/enzymatic-assay-of-hexokinase.html
30. Bergmeyer, H-U. Methods of enzymatic analysis. Elsevier; 1965.
31. 2-NBDG as a fluorescent indicator for direct glucose uptake measurement. J Biochem Biophys Methods. 2005; 64:207–15. [PubMed: 16182371]
32. Park SG, Lee JH, Lee WA, Han KM. Biologic correlation between glucose transporters, hexokinase-II, Ki-67 and FDG uptake in malignant melanoma. Nuclear medicine and biology. 2012; 39:1167–72. [PubMed: 22901702]
33. Kafri R, Levy J, Ginzberg MB, Oh S, Lahav G, Kirschner MW. Dynamics extracted from fixed cells reveal feedback linking cell growth to cell cycle. Nature. 2013; 494:480–3. [PubMed: 23446419]
34. Boussemart L, Malka-Mahieu H, Girault I, Allard D, Hemmingsson O, Tomasic G, et al. eIF4F is a nexus of resistance to anti-BRAF and anti-MEK cancer therapies. Nature. 2014; 513:105–9. [PubMed: 25079330]
35. Silva JM, Bulman C, McMahon M. BRAFV600E cooperates with PI3K signaling, independent of AKT, to regulate melanoma cell proliferation. Molecular cancer research: MCR. 2014; 12:447–63. [PubMed: 24425783]
36. Clark DE, Errington TM, Smith JA, Frierson HF Jr, Weber MJ, Lannigan DA. The serine/threonine protein kinase, p90 ribosomal S6 kinase, is an important regulator of prostate cancer cell proliferation. Cancer research. 2005; 65:3108–16. [PubMed: 15833840]
37. Kang S, Elf S, Lythgoe K, Hitosugi T, Taunton J, Zhou W, et al. p90 ribosomal S6 kinase 2 promotes invasion and metastasis of human head and neck squamous cell carcinoma cells. The Journal of clinical investigation. 2010; 120:1165–77. [PubMed: 20234090]
38. Wolchok JD, Hoos A, O'Day S, Weber JS, Hamid O, Lebbe C, et al. Guidelines for the evaluation of immune therapy activity in solid tumors: immune-related response criteria. Clinical cancer research: an official journal of the American Association for Cancer Research. 2009; 15:7412–20. [PubMed: 19934295]
39. Haq R, Shoag J, Andreu-Perez P, Yokoyama S, Edelman H, Rowe GC, et al. Oncogenic BRAF regulates oxidative metabolism via PGC1alpha and MITF. Cancer cell. 2013; 23:302–15. [PubMed: 23477830]
40. Yamada K, Brink I, Bisse E, Epting T, Engelhardt R. Factors influencing [F-18] 2-fluoro-2-deoxy-D-glucose (F-18 FDG) uptake in melanoma cells: the role of proliferation rate, viability, glucose transporter expression and hexokinase activity. The Journal of dermatology. 2005; 32:316–34. [PubMed: 16043894]
41. Paraiso KH, Fedorenko IV, Cantini LP, Munko AC, Hall M, Sondak VK, et al. Recovery of phospho-ERK activity allows melanoma cells to escape from BRAF inhibitor therapy. British journal of cancer. 2010; 102:1724–30. [PubMed: 20531415]

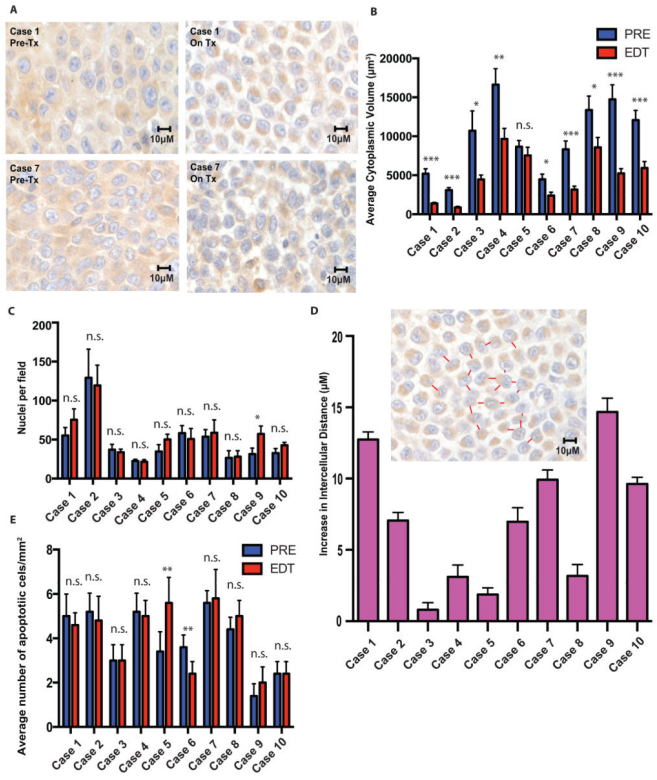

Figure 1.

BRAF inhibition induces a significant decrease in cell volume in treated human melanoma tumors. A–B, A significant reduction in mean cytoplasmic volume is observed in the majority of biopsies of patient tumors after commencement of BRAFi therapy C, without a significant decrease in mean number of nuclei per HPF. D, The majority of cases showed a large increase in average intercellular distance after commencement of therapy. E, a significant increase in number of apoptotic nuclei was not observed in the majority of cases. *, $p < 0.05$; **, $p < 0.01$; ***, $p < 0.001$.

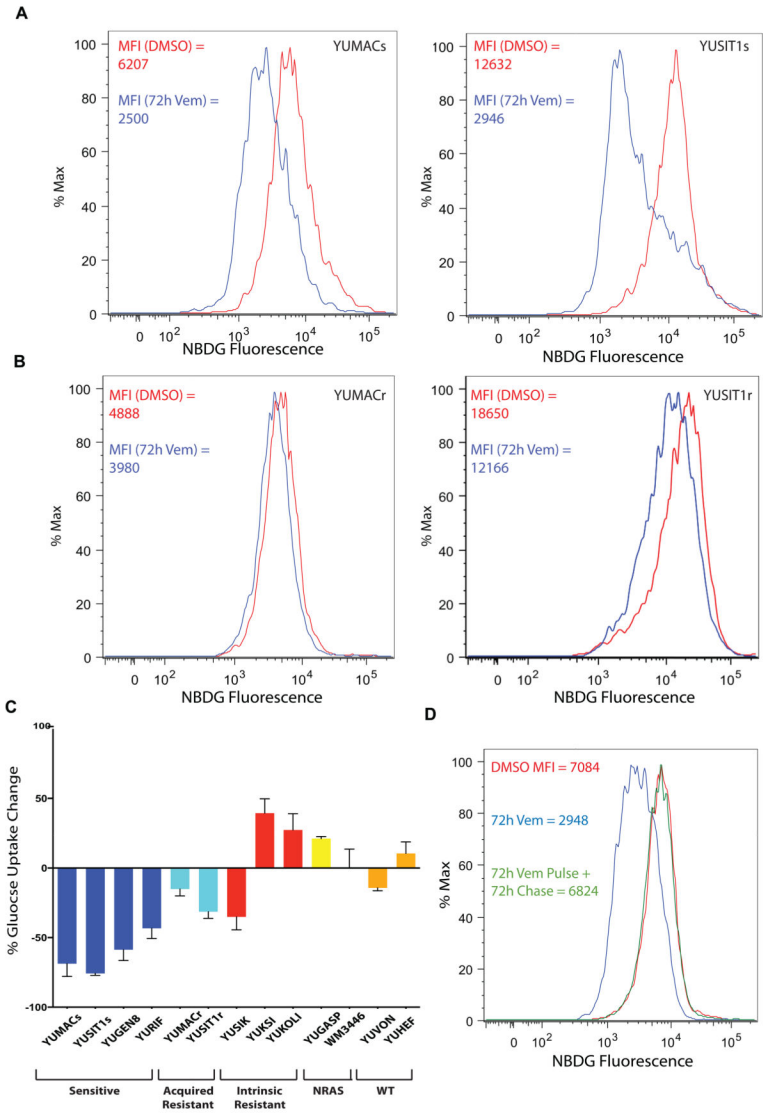

Figure 2.

Vemurafenib causes a decrease in glucose uptake in drug-sensitive but not resistant lines. A, Treatment with 3μM Vemurafenib causes a decrease in glucose uptake as assessed by flow cytometry using the fluorescent glucose analog 2-NBDG reaching maximum decrease by 72 hours. B, Acquired-resistant lines (e.g. YUMACr) that have been serially passaged in 5μM Vemurafenib show a much lower decrease in glucose uptake than drug-naive lines (e.g. YUMACs). C, Changes in glucose uptake with BRAF inhibition mirror resistance status and are genotype-specific. D, Glucose uptake loss due to vemurafenib treatment is reversible. All cells were incubated in 3μM vemurafenib or DMSO vehicle for 72 hours. After 72 hours, the pulse-chase group had vemurafenib-supplemented media aspirated, was washed with PBS, and re-supplied with normal media supplemented with vehicle.

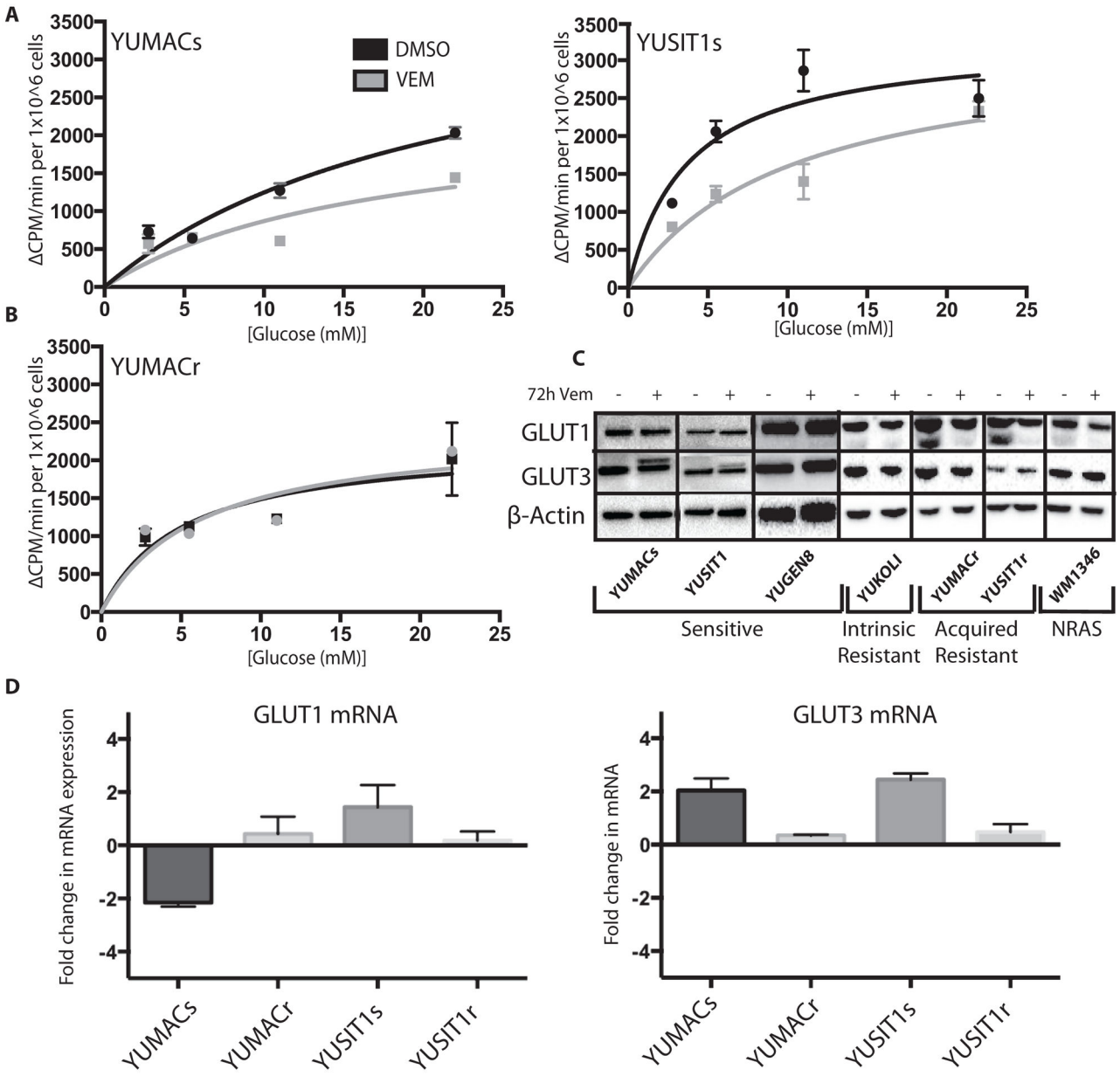

Figure 3.

Vemurafenib induces a decrease in transmembrane glucose uptake per cell. A, 3μM Vemurafenib (+) incubation induces a decrease in transport of the non-phosphorylatable glucose analog 3-OMG normalized to cell count in sensitive lines but not B, acquired resistant lines relative to DMSO (−) after 72 hours. C, Vemurafenib treatment does not cause a significant decrease in GLUT1 or GLUT3 proteins levels in sensitive or resistant lines by 72 hours. D, Vemurafenib does not induce a significant change in GLUT1 or GLUT3 mRNA levels after 72 hours as detected by RT-qPCR.

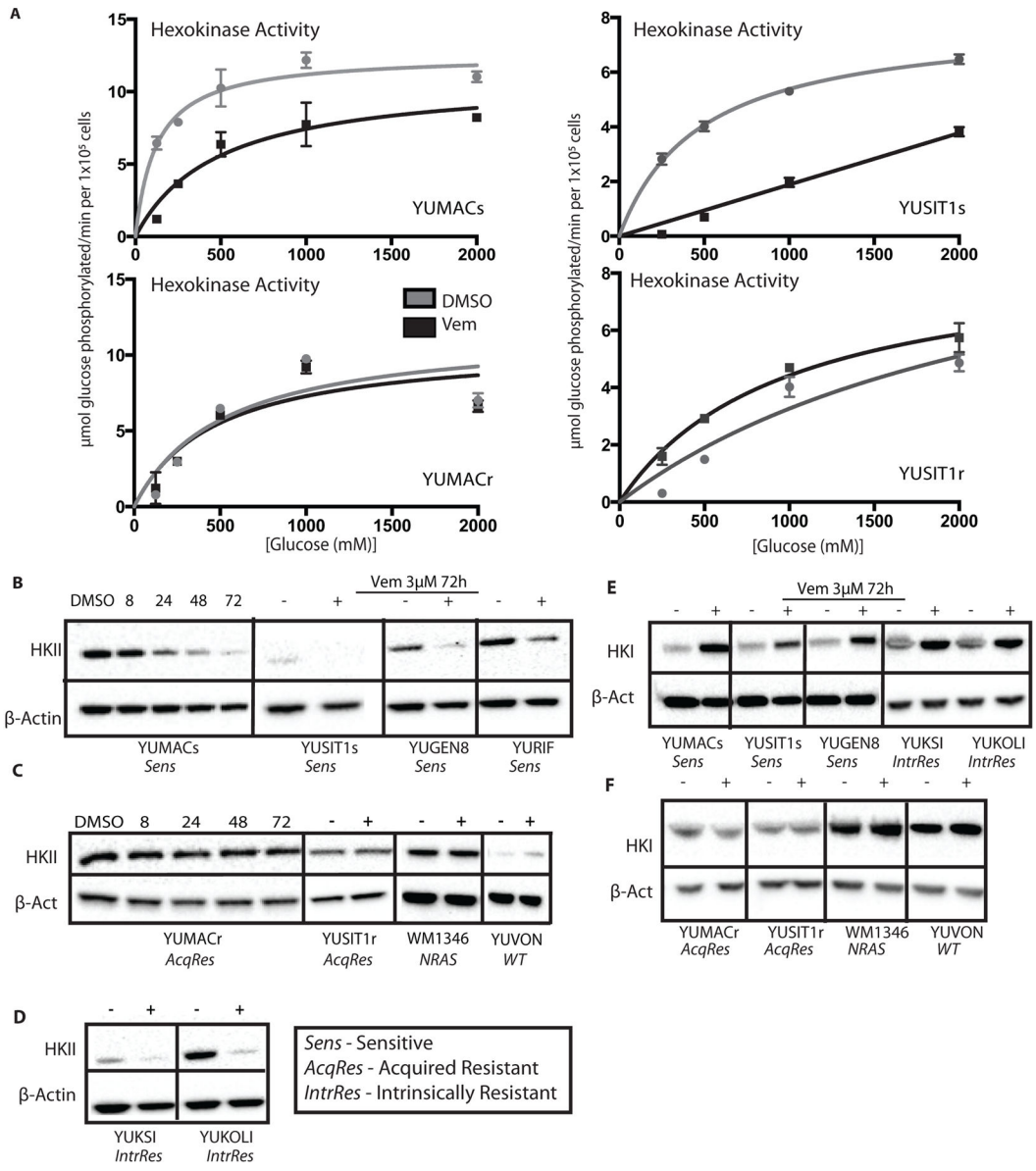

Figure 4.

Vemurafenib induces significant loss of HKII in both sensitive and intrinsically resistant lines. A, 3µM Vemurafenib induces a decrease in overall hexokinase activity per cell after 72 hours in sensitive cell lines B, Vemurafenib (+) induces near complete loss of HKII in sensitive but not C, acquired resistant or non-BRAF cell lines at 72 hours relative to DMSO (−). D, Intrinsically resistant cell lines show a decrease in HKII comparable to sensitive cell lines. E, Sensitive and intrinsically resistant lines show a significant increase in HKI with Vemurafenib treatment by 72 hours that is not observed in acquired resistant or non-*BRAF* mutant lines, F.

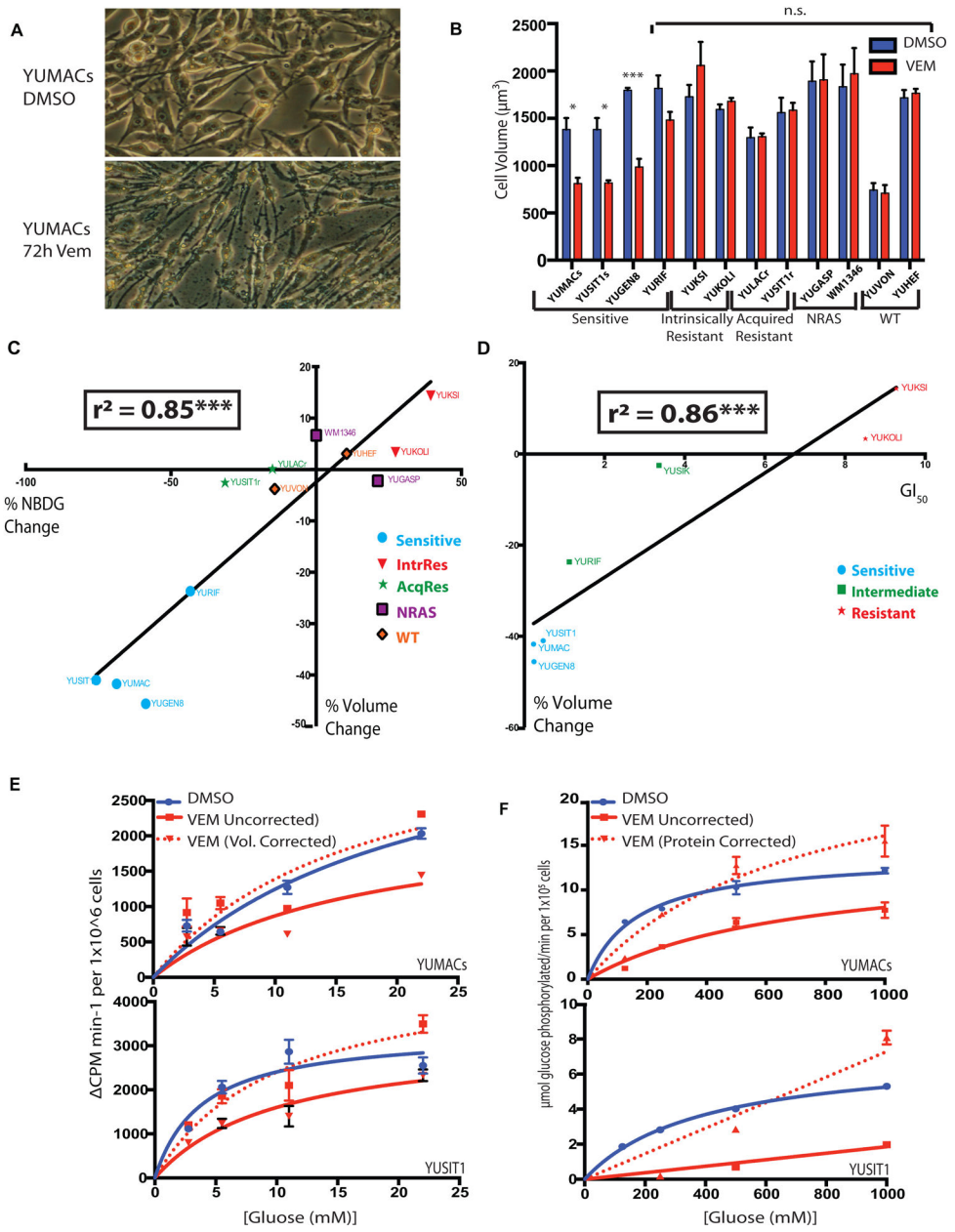

Figure 5.

3µM Vemurafenib induces a cellular volume decrease in sensitive lines which largely accounts for alterations in glucose uptake per cell. A, Adherent sensitive but not resistant cell lines show visual decrease in cell size by light microscopy. B, Vemurafenib-sensitive but neither acquired nor intrinsically resistant cell lines show a decrease in total cell volume with treatment as assessed by Coulter Counter. C, Changes in cell volume show a strongly significant correlation with changes in measured glucose uptake ($r^2 = 0.8483$, $p < 0.01$). D, Changes in cell size also show a strong correlation with Vemurafenib GI_{50} for mutant BRAF lines ($r^2 = 0.8568$, $p < 0.01$). E, Changes in transmembrane glucose transport are largely

abrogated when corrected for changes in cell volume. F, Changes in hexokinase activity are also largely abrogated when normalized to whole lysate protein concentration.

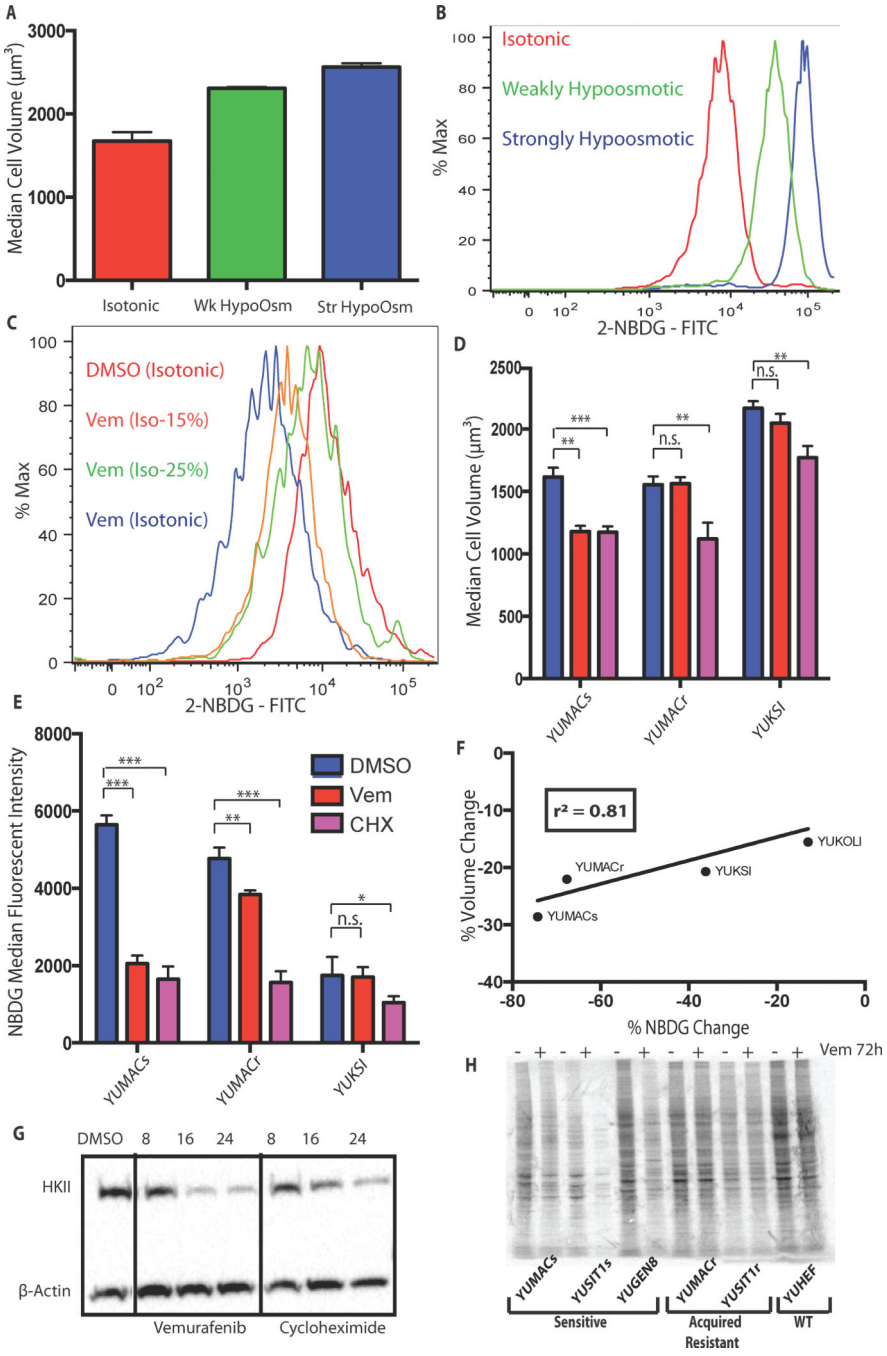

Figure 6.

Glucose uptake is greatly affected by changes cell volume. A, Decreasing solution osmolarity while incubating with 2-NBDG causes both an increase in cell volume and B, 2-NBDG uptake that is osmolarity-dependent. The isotonic condition has a total concentration of 289 mOsm/L, while the weakly and strongly hypoosmotic conditions have concentrations of 144.5 mOsm/L and 72.25 mOsm/L respectively. C, Incubation of 3μM vemurafenib-treated cells in hypoosmotic 2-NBDG solution restored glucose uptake to the same level as isotonic 2-NBDG control at 217 mOsm/L. D. Inhibition of protein translation with 50 μg/mL

cycloheximide induces a decrease in both cell volume and E, glucose uptake at 24 hours with F, a relationship similar to 3μM vemurafenib ($r^2 = 0.8153$, $p = 0.097$). G, Inhibition of translation with cycloheximide produces comparable loss of HKII to Vemurafenib by 24h. H, ^{35}S methionine labeling shows that incubation of vemurafenib sensitive but not resistant lines for 72h with 3μM reduced total new protein synthesis, *, $p < 0.05$; **, $p < 0.01$; ***, $p < 0.001$.